Original Article

Ferumoxytol-enhanced 4D multiphase, steady-state imaging with magnetic resonance in congenital heart disease: ventricular volume and function across 2D and 3D software platforms

Takegawa Yoshida[1], Joseph J. Chen[1,2], Bill Zhou[1,2], J. Paul Finn[1,3], Peng Hu[1,3], Kim-Lien Nguyen[1,2,3]^

[1]Diagnostic Cardiovascular Imaging Research Laboratory, David Geffen School of Medicine at University of California, Los Angeles, Los Angeles, CA, USA; [2]Division of Cardiology, David Geffen School of Medicine at University of California, Los Angeles and Veterans Affairs Greater Los Angeles Healthcare System, Los Angeles, CA, USA; [3]Physics and Biology in Medicine Graduate Program at University of California, Los Angeles, CA, USA

Contributions: (I) Conception and design: KL Nguyen, P Hu; (II) Administrative support: None; (III) Provision of study materials or patients: JP Finn; (IV) Collection and assembly of data: T Yoshida, JJ Chen, B Zhou; (V) Data analysis and interpretation: All authors; (VI) Manuscript writing: All authors; (VII) Final approval of manuscript: All authors.

Correspondence to: Kim-Lien Nguyen, MD. Diagnostic Cardiovascular Imaging Research Laboratory, David Geffen School of Medicine at University of California, Los Angeles, Veterans Affairs Greater Los Angeles Healthcare System, 11301 Wilshire Blvd, MC 111E, Los Angeles, CA 90073, USA. Email: klnguyen@ucla.edu.

Background: Quantitative ventricular volumetry and function are important in the management of congenital heart disease (CHD). Ferumoxytol-enhanced (FE) 4D multiphase, steady state imaging with contrast enhancement (MUSIC) enables high-resolution, 3D cardiac phase-resolved magnetic resonance imaging (MRI) of the beating heart and extracardiac vessels in a single acquisition and without concerns about renal impairment. We aim to evaluate the semi-automatic quantification of ventricular volumetry and function of 4D MUSIC MRI using 2D and 3D software platforms.

Methods: This HIPAA-compliant and IRB-approved study prospectively recruited 50 children with CHD (3 days to 18 years) who underwent 4D MUSIC MRI at 3.0T between 2013–2017 for clinical indications. Each patient was either intubated in the neonatal intensive care unit (NICU) or underwent general anesthesia at MRI suite. For 2D analysis, we reformatted MUSIC images in Digital Imaging and Communications in Medicine (DICOM) format into ventricular short-axis slices with zero interslice gap. For 3D analysis, we imported DICOMs into a commercially available 3D software platform. Using semi-automatic thresholding, we quantified biventricular volume and ejection fraction (EF). We assessed the bias between MUSIC-derived 2D *vs.* 3D measurements and correlation between MUSIC *vs.* conventional 2D balanced steady-state free precession (bSSFP) cine images. We evaluated intra- and inter-observer agreement.

Results: There was a high degree of correlation between MUSIC-derived volumetric and functional measurements using 2D *vs.* 3D software (r=0.99, P<0.001). Volumes derived using 3D software platforms were larger than 2D by 0.2 to 2.0 mL/m^2 whereas EF measurements were higher by 1.2–3.0%. MUSIC volumetric and functional measures derived from 2D and 3D software platforms corresponded highly with those derived from multi-slice SSFP cine images (r=0.99, P<0.001). The mean difference in volume for reformatted 4D MUSIC relative to bSSFP cine was 1.5 to 3.9 mL/m^2. Intra- and inter-observer reliability was excellent.

Conclusions: Accurate and reliable ventricular volumetry and function can be derived from FE 4D MUSIC MRI studies using commercially available 2D and 3D software platforms. If fully validated in multicenter studies, the FE 4D-MUSIC pulse sequence may supercede conventional multislice 2D cine

^ ORCID: 0000-0002-8854-2976.

cardiovascular MRI acquisition protocols for functional evaluation of children with complex CHD.

Keywords: Congenital heart disease (CHD); cardiovascular magnetic resonance imaging; cardiac function; ferumoxytol; 4D imaging

Submitted Dec 29, 2021. Accepted for publication May 07, 2022.
doi: 10.21037/qims-21-1243
View this article at: https://dx.doi.org/10.21037/qims-21-1243

Introduction

Reliable quantification of cardiac volumetry and function is vital for the planning and timing of surgical intervention in patients with complex congenital heart disease (CHD) (1,2). Contrast-enhanced magnetic resonance angiography (CE-MRA) with supplemental multislice 2D cine magnetic resonance imaging (MRI) has long served as the workhorse for visualizing complex intracardiac anatomy, extracardiac vascular connections, and quantification of ventricular volumetry and function (3). Conventional 3D CE-MRA under general anesthesia typically requires breath-holding by suspending positive pressure ventilation during the passage of a gadolinium-based contrast agent (GBCA). Moreover, multi-slice cine image acquisition requires numerous, additional sequential breath-holds, as well as advanced operator skills to prescribe appropriate imaging planes and optimize acquisition parameters. The aforementioned requirements add complexity to the MRI workflow and often result in prolonged and unpredictable examination times under anesthesia. 4D multiphase, steady state imaging with contrast enhancement (MUSIC) (4) and its ROCK-MUSIC (Rotating Cartesian K-space) variants (5-7) were developed to overcome these challenges.

4D MUSIC is a cardiac- and respiratory-gated, high bandwidth, spoiled gradient recalled echo (GRE) sequence that acquires high resolution, 3D volumetric data over a large field-of-view (FOV) and over multiple phases of the cardiac cycle, during uninterrupted positive pressure ventilation with general anesthesia. Prior studies reported larger end-diastolic ventricular volumes derived from noncontrast balanced steady-state free precession (bSSFP) cine images relative to those derived from 2D spoiled-GRE (8,9). Although bSSFP cine imaging has superceded GRE at 1.5 T due to its superior image contrast and faster image acquisition, at 3.0T, bSSFP images are often undermined by off-resonance and flow artifacts (10,11). 4D MUSIC leverages the higher signal available at 3.0T in combination with ferumoxytol (Feraheme®, Covis Pharma, Waltham, MA, USA) for improved myocardial-to-blood pool contrast in steady-state cine imaging. Ferumoxytol has an intravascular half-life of 14–15 h, an r_1 (9.0 $mM^{-1}s^{-1}$, 3.0T) that is higher than those of commercially available GBCAs, and is well tolerated in patients with premature or impaired renal function (4,12).

Preliminary work with 4D MUSIC MRI has demonstrated improved visualization of intracardiac anatomy relative to 2D multi-slice cardiac cine imaging (6) whereas the additive clinical value of ferumoxytol-enhanced 4D MUSIC for CHD imaging is simplification of the imaging protocol (13). However, the optimal post-processing software for routine derivation of cardiac volumetry and function has not been established for 4D MUSIC. Because 4D MUSIC images in DICOM (Digital Imaging and Communications in Medicine) format can be reformatted and interrogated in any arbitrary imaging plane, accurate and reliable quantification of ventricular volumes and ejection fraction is feasible. In this work, we aim to evaluate the accuracy and reliability of semi-automatic quantification of ventricular volumetry and function for 4D MUSIC MRI using commercially available 2D and 3D image analysis software. We present the following article in accordance with the GRRAS reporting checklist (available at https://qims.amegroups.com/article/view/10.21037/qims-21-1243/rc).

Methods

Study population

This retrospective study was approved by the Institutional Ethics Board at University of California, Los Angeles, USA and was compliant with the Health Insurance Portability and Accountability Act. The study was conducted in accordance with the Declaration of Helsinki (as revised in 2013). All patients or their legal guardians gave written informed consent. We included 50 consecutive children with CHD (age 2 days to 18 years, 25 males) who underwent

Table 1 Patient characteristics (n=50)

Characteristics	n [%]
Male gender	25 [50]
Age (range)	3 days to 18 years
Heart rate (bpm)†	122.6±30.6† [60–173]
Primary diagnosis	
Tetralogy of Fallot	18 [36]
Aortic arch abnormality	14 [28]
Hypoplastic/interrupted aortic arch	9 [18]
Complete/incomplete vascular ring	5 [10]
Bicuspid aortic valve	3 [6]
Patent ductus arteriosus	2 [4]
Truncus arteriosus	2 [4]
Anomalous pulmonary venous connection	2 [4]
Transposition of great vessels	2 [4]
Ventral septal defect	1 [2]
Other	6 [12]
Anomalous coronary artery	2 [4]
Aberrant subclavian artery	1 [2]
Hypertrophic cardiomyopathy	1 [2]
Myocardial thinning	1 [2]
Normal	1 [2]

†, values are reported as mean ± standard deviation.

clinically-indicated 4D MUSIC MRI between December 2013 to November 2017 at a quaternary inpatient hospital setting. Primary CHD diagnoses are summarized in *Table 1*.

Image acquisition

Detailed image acquisition has been previously described. Briefly, we acquired all images using a clinical whole body 3.0Tesla MRI scanner (Magnetom TIM Trio, Siemens Medical Solutions, Erlangen, Germany). In patients who were not already intubated in the neonatal intensive care unit or pediatric intensive care unit, intubation was performed after induction of general anesthesia in the MRI suite. We continuously monitored the vital signs throughout the exam and for up to 30 minutes after ferumoxytol infusion using an MRI compatible monitoring system (InVivo Research, Orlando, FL). We administered ferumoxytol as a slow intravenous infusion (4 mg/kg, at 8–10× dilution) at a rate <5 mg Fe/s. During steady-state ferumoxytol distribution, 4D MUSIC images were acquired during uninterrupted, positive pressure ventilation, using the airway pressure signal for respiratory gating and either the electrocardiogram (ECG) or pulse oximetry signal for cardiac-gating. The airway pressure signal was used for respiratory gating because the ventilator airway pressure signal provides a more consistent respiratory pattern, which makes breath-holds (or suspension of the ventilator) unnecessary during the 4D MUSIC acquisition. Typical sequence parameters were: repetition time (TR) =2.9 ms, echo time (TE) =0.9 ms, flip angle =25°, 3D isotropic resolution =0.6–0.9 mm, 5–9 cardiac phases, scan time 4–12 min, temporal resolution =65–95 ms. In 10 patients, we acquired conventional multislice 2D cine images using the balanced steady-state free precession (bSSFP) pulse sequence after ferumoxytol infusion. bSSFP images served as the reference comparison because this is the clinical MRI standard for quantification of ventricular volumes and function. The sequence parameters were: TR =3.2 ms, TE =1.6 ms, flip angle =65°, slice thickness 3–5 mm with 1–6 mm interslice gap, at least 25 cardiac phases, temporal resolution 40–60 ms.

Image analysis

Image analysis was performed using both 2D and 3D software platforms to determine whether the use of 3D software platforms offered incremental advantages compared to 2D platforms. It is well-recognized that derivation of volumetric data using 3D software platforms can be labor-intensive. Two trained readers (BZ, TY) performed the image analysis without having knowledge of the clinical diagnoses. Both were trained to perform ventricular quantification by a cardiovascular MR reader (KLN) with subspecialty fellowship training and >8 years' experience in cardiovascular MRI. Readers used a separate training dataset prior to quantification of the study dataset.

2D image analysis

We reformatted 4D MUSIC DICOM data into ventricular short-axis (slice thickness of 4 mm and zero interslice gap) and long-axis slices using QMass® (Medis, Leiden, Netherlands). To properly define the most basal slice and avoid foreshortening, we cross-referenced the valve plane and ventricular apex to avoid segmentation errors. We defined the end-systolic (ES) and end-diastolic (ED) phases

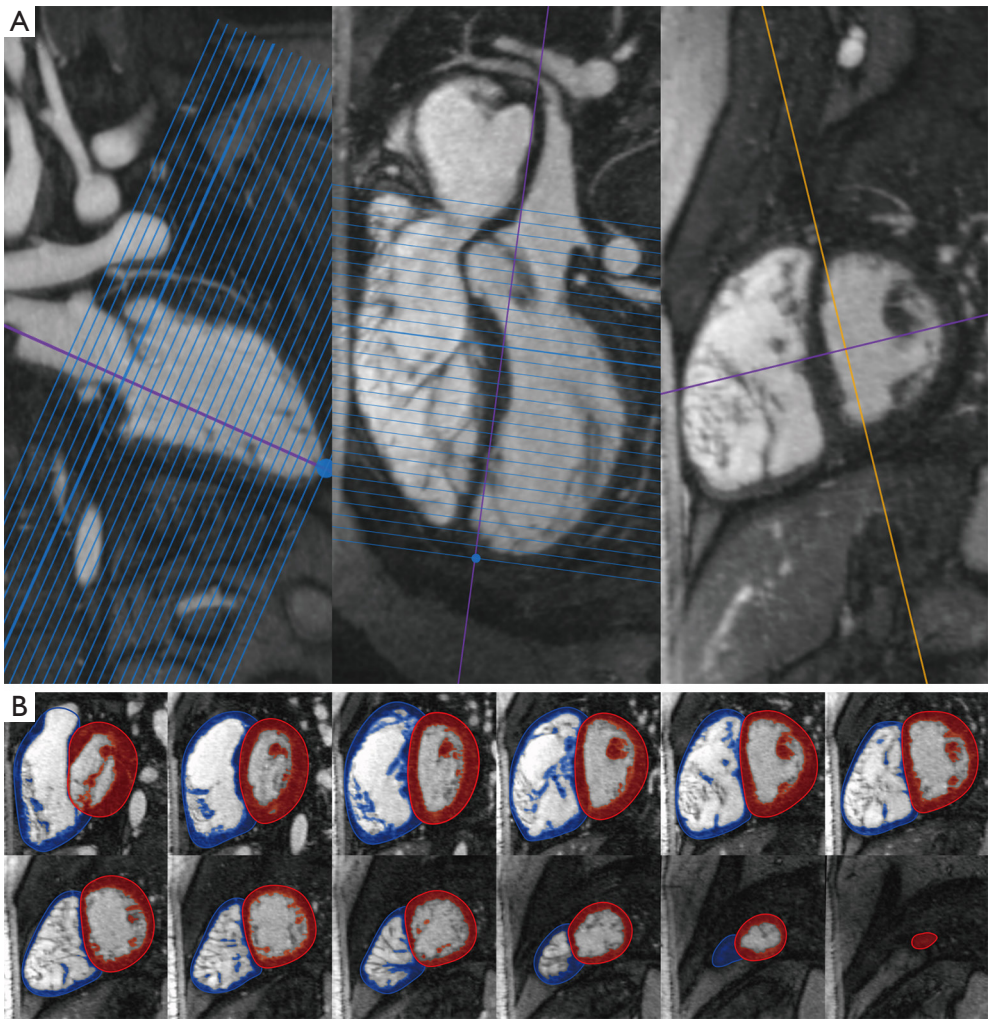

Figure 1 Reformatting of 4D MUSIC images. (A) To derive multislice 2D images for quantification of volumes and ejection fraction, we reformatted 4D MUSIC images into multislice short-axis images using orthogonal, long-axis images. The blue lines each represent a 2D short axis slice (A, right panel) that is perpendicular to the long-axis image. The purple and yellow lines represent orthogonal planes. (B) We manually defined the ventricular epicardial contours from base to apex followed by semi-automated segmentation of the right (B, blue overlay) and left ventricles (B, red overlay). MUSIC, multiphase, steady-state imaging with contrast.

using the long-axis image and the mid-left ventricular short-axis image. In some patients, the ES and ED phases differed for right ventricle (RV) and left ventricle (LV) due to abnormal cardiac conduction. We traced the epicardial contours for both RV and LV in ES and ED, from the basal to apical slice (*Figure 1*). We defined the LV contours from the apex to the level of the left ventricular outflow tract (LVOT) and aortic valve. The RV contours extended from the RV apex to the right ventricular outflow tract (RVOT) and pulmonary valve. The septum was considered to be part of the LV. The segmentation software calculated the ventricular volumes based on a semi-automatic pixel-intensity algorithm. In brief, voxels within the traced epicardial contour were differentiated into myocardium versus blood pool based on voxel signal intensity; dark voxels were treated as myocardial tissue while bright voxels from the contrast agent were considered blood pool. The trabeculae and papillary muscles were purposely excluded from the blood pool. The automatic thresholding can be manually adjusted, and voxels can be painted over as needed to account for inappropriate thresholding or artifacts such as postoperative sternotomy wires. After thresholding, the regions of interest were multiplied by the slice thickness and summed across all tracings from base to apex to calculate the

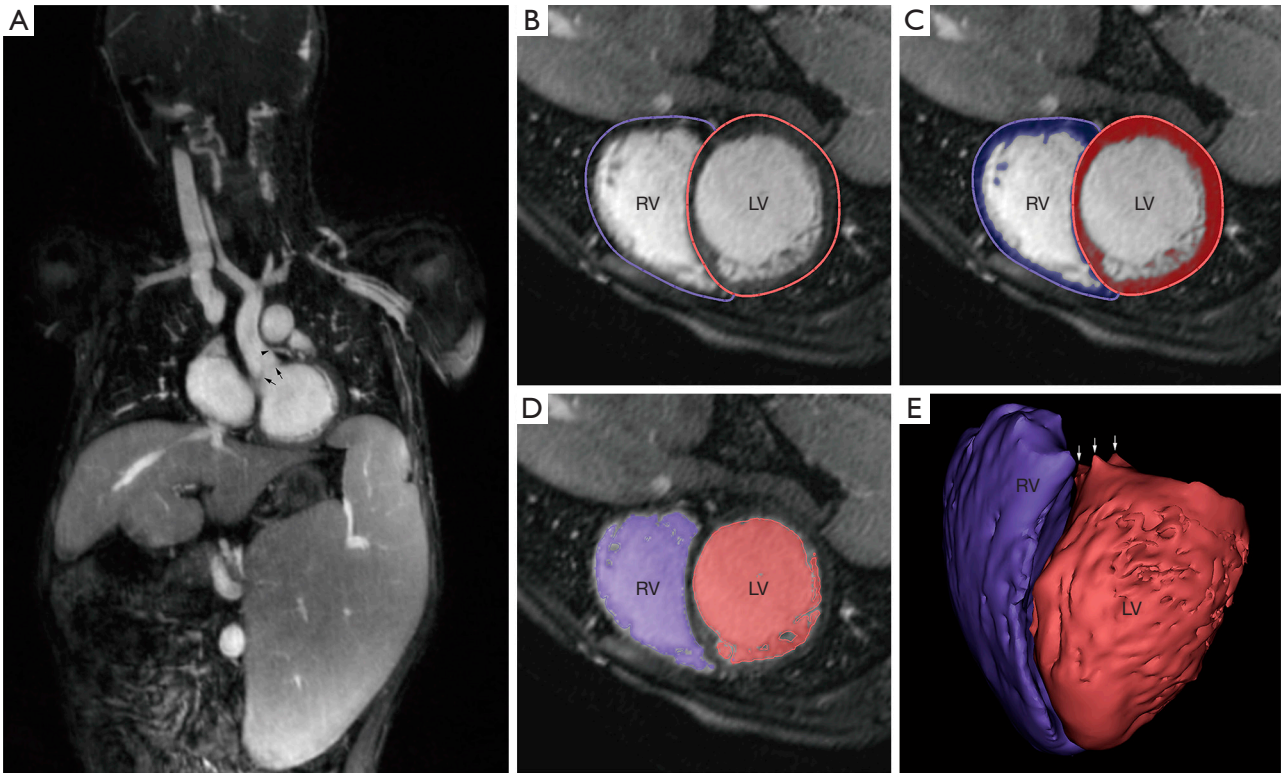

Figure 2 Representative 4D MUSIC images used for quantification of ventricular volumetry and function. (A) 4D MUSIC images belonging to a 17-month-old boy (11.4 kg) show sharp intra-cardiac borders and clear definition of the aortic valve leaflets (A, black arrow), and proximal left anterior descending artery (A, black arrowhead). (B) Multiplanar reformat of ventricular short axis show epicardial borders and (C) segmented endocardial borders. (D) To obtain 3D quantification of volumes and ejection fraction, we manually segmented the blood pool of the cardiac chambers using seeds and user-defined thresholds, (E) and the software generated a 3D reconstruction of the heart based on the segmentation. The white arrows reflect the ventricular side of the aortic valve leaflet. LV, left ventricle; RV, right ventricle; MUSIC, multiphase steady-state imaging with contrast.

ventricular volumes. Volumes were indexed to body surface area using the Dubois-Dubois formula. Ejection fraction (EF) was calculated by the formula [end-diastolic volume (EDV) – end-systolic volume (ESV)]/EDV × 100%.

3D image analysis

The ES and ED phases were selected and exported using OsiriX (Pixmeo, Geneva, Switzerland). We used the coronal slice with the highest number of visualized cardiac chambers as reference and examined each frame. The ES and ED were defined based on the smallest and largest ventricular chamber size, respectively. Then, the DICOM data were directly imported into Mimics Innovation Suite® (Materialise, Leuven, Belgium) to generate axial, coronal, and sagittal views. We applied manual thresholding to the ED images by selecting the lowest cutoff intensity for inclusion of voxels into the final 3D reconstruction of the cardiac chambers. The consensus standard between the two readers was to maximize the blood pool while minimizing inclusion of trabeculae and papillary muscles. After thresholding, we placed labeled "seeds" in the LV, RV, left atrium, right atrium, aorta, and pulmonary artery across all three views. Using a region-growing algorithm, we propagated the seeds along voxels of similar signal intensity until a different seed is encountered. Extra seeds were placed along the valves to define the atrio-ventricular and ventriculo-arterial connections. The end result was a color-coded segmentation of blood pool, cardiac chambers, and major vessels, which we reconstructed into a 3D model of the heart for quantification of volumetry and function (*Figure 2*). We repeated the same process for the ES phase using the thresholding value determined from the ED

phase. We indexed the volume based on body surface area using the Dubois-Dubois formula and calculated the EF using the formula (EDV – ESV)/EDV × 100%.

One reader (BZ) performed the intra-observer agreement evaluation by reanalyzing 10 random patients across both software platforms. The reader (BZ) was blinded to the initial results and the re-analysis interval was one week. To determine inter-observer agreement, a second reader (TY) also independently analyzed 10 random patients using both software platforms. The readers were blinded to each other's phase and slice selection, thresholding values, as well as volumetry and function results.

Statistical analysis

We tested accuracy and reliability by comparing measures of volumetry and function between 4D MUSIC relative to conventional SSFP cine images. To define accuracy for 4D MUSIC across 2D (Qmass) relative to 3D (Mimics) software platforms, we assessed the following: (I) correlation between measures of 4D MUSIC-derived volumetry and cine SSFP-derived values; (II) correlation between 2D relative to 3D software analysis of 4D MUSIC for end-systolic volume (ESV), end-diastolic volume (EDV), and ejection fraction (EF); (III) differences between 2D-relative to 3D-software derived 4D MUSIC measures of ESV, EDV, and EF. To assess reliability, we performed intra- and interobserver reliability correlation across 2D and 3D software platforms. Data were tested for normality using the Shapiro-Wilk test. Group differences were tested using the Wilcoxon-rank-sum test. Correlation and agreement were tested using Spearman's rho and Bland-Altman plots, respectively. Intra- and inter-observer reliability were tested using intraclass correlation coefficient (ICC) and coefficient of variation (CV). Statistical analyses were conducted using SPSS 19.0 (IBM SPSS, Chicago, IL, USA) and MedCalc 17.2 (MedCalc Software, Ostend, Belgium). Statistical significance was considered to have a P value <0.05. Continuous data are reported as median with interquartile range and categorical data are reported as absolutes and percentages.

Results

We enrolled 50 children with CHD [age range 3 days – 18 years, median 9.9 (interquartile 0.2–48.7) months, male 50% (n=25)] in the study. Patient characteristics are outlined in *Table 1*. No ferumoxytol-related adverse events occurred. All patients remained hemodynamically stable throughout the duration of the scan. Typical temporal resolution ranged from 65–95 ms. Video S1 provides a sample illustration of 4D MUSIC images. There were no statistically significant differences in biventricular ESV (P=0.85–0.93), EDV (P=0.93–0.97), and EF (P=0.12–0.51) quantification derived from 4D MUSIC MRI using 2D or 3D software platforms. On average, segmentation using 3D software required 5 to 20 minutes per case whereas segmentation using 2D software took <5 minutes.

Accuracy between 4D MUSIC measures of volumetry and function relative to conventional bSSFP cine

There was good to excellent correlation between 4D MUSIC measures of ESV, EDV, and EF across both 2D and 3D software platforms, and with those derived from bSSFP cine images (*Table 2*). Bland-Altman analyses of 4D MUSIC (using 2D software) *vs.* conventional bSSFP cine are shown in *Figure 3*. In general, correlation strength was stronger for volumetry (ESV, EDV) than for functional measurements (EF). 2D software analysis of reformatted 4D MUSIC images showed very strong positive correlation with reference bSSFP cine images. Spearman's rho for all volumetric measurements were >0.95 (P<0.001). In contrast, correlations in LVEF and RVEF were strong, but the strength of correlation was lower with rho values of 0.87 (P=0.001) and 0.77 (P=0.009), respectively. Volumes derived from reformatted 4D MUSIC images using 2D software tended to be higher than those from bSSFP cine images. The mean difference in volume for reformatted 4D MUSIC relative to bSSFP cine was +1.5 to +3.9 mL/m^2 (*Figure 3*).

The correlations between 4D MUSIC ESV, EDV, and EF derived from 3D software had weaker correlation with bSSFP cine analysis (*Table 2*). Spearman's rho for all volumetric measurements were >0.95 (P<0.001), whereas rho values for biventricular EF were moderate in strength: LVEF (r=0.68, P=0.029), RVEF (r=0.77, P=0.009). Quantification of 4D MUSIC images using the 3D software platform resulted in larger volumes relative to those derived from bSSFP cine images by an average of +2.15 to +5.2 mL/m^2 (*Figure 4*).

Correlation between 2D (Qmass) relative to 3D (Mimics) software platforms for 4D MUSIC MRI quantification of volumetry and function

Quantification of cardiac volumetry and function using 2D and 3D software platforms demonstrated very strong

Table 2 Correlation between 4D MUSIC and bSSFP-derived measures of cardiac chamber volumetry and function

Variables	bSSFP cine	4D MUSIC 2D reformats†	2D reformats *vs.* bSSFP (rho)‡	4D MUSIC 3D analysis†	3D *vs.* bSSFP (rho)‡
LVEDV (mL/m^2)	28.7 (19.0–41.6)	28.7 (19.4–47.3)	0.99	26.8 (20.8–49.9)	0.98
LVESV (mL/m^2)	11.1 (5.3–19.5)	11.1 (6.1–20.6)	0.98	10.8 (6.0–23.4)	0.95
LVEF (%)	59.0 (57.1–64.0)	57.7 (54.6–64.3)	0.87	58.4 (52.7–69.1)	0.68
RVEDV (mL/m^2)	34.6 (17.8–58.2)	35.2 (9.6–66.0)	0.98	34.3 (19.4–69.4)	0.98
RVESV (mL/m^2)	17.7 (7.0–21.8)	19.1 (6.9–24.9)	0.95	18.6 (6.0–27.4)	0.98
RVEF (%)	59.4 (51.8–63.1)	58.0 (50.4–64.5)	0.77	58.4 (52.7–66.0)	0.77

†, QMass (MedisSuite) was used for 2D image analysis. Mimics (Materialise) was used for 3D image analysis. ‡, Spearman's rho values are reported. Ventricular volume and ejection fraction values are reported as median and IQR. All P values were <0.05. MUSIC, multiphase, steady-state imaging with contrast; bSSFP, balanced steady-state free precession; LVEDV, left ventricular end-diastolic volume; LVEF, left ventricular ejection fraction; LVESV, left ventricular end-systolic volume; RVEDV, right ventricular end-diastolic volume; RVESV, right ventricular end-systolic volume; RVEF, right ventricular ejection fraction; IQR, interquartile range.

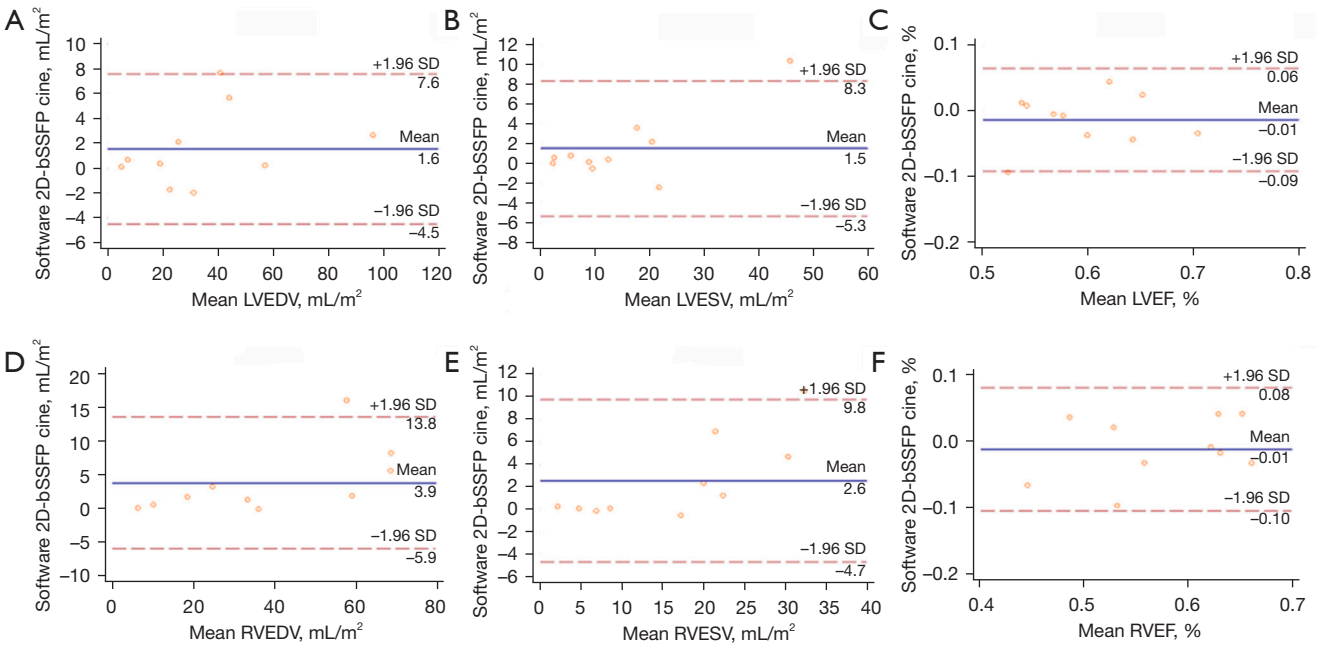

Figure 3 Comparison of Software^{2D} (Qmass) analysis of 4D MUSIC and multislice bSSFP cine images for measures of volumetry and function. Bland-Altman plots of (A) LVEDV, (B) LVESV, (C) LVEF, (D) RVEDV, (E) RVESV, and (F) RVEF. The mean values between Software^{2D} (Qmass) and bSSFP cine are on the x-axis and the absolute difference [Software^{2D} (Qmass)-bSSFP cine] are on the y-axis. bSSFP, balanced steady-state free precession; LVEDV, left ventricular end-diastolic volume; LVESV, left ventricular end-systolic volume; LVEF, left ventricular ejection fraction; RVEDV, right ventricular end-diastolic volume; RVESV, right ventricular end-systolic volume; RVEF, right ventricular ejection fraction; MUSIC, multiphase, steady-state imaging with contrast.

correlation (*Table 3*). Spearman's rho values were all >0.90 (all P values <0.001). Correlation coefficients were stronger for ventricular volumes than for calculated EF. Bland-Altman analyses for 2D *vs.* 3D software are shown in *Figure 4*. Overall, the 3D software produced slightly higher volumetric values and EF than the 2D software, which is expected. For volumetric measurements, 3D analysis produced volumes that were larger by a range of 0.2 to 2.0 mL/m^2. For functional measurements, 3D analysis produced values that were higher by a range of 1.2–3.0%. For the purpose of EF and ventricular volume analysis, we did not observe any additional advantage to using 3D

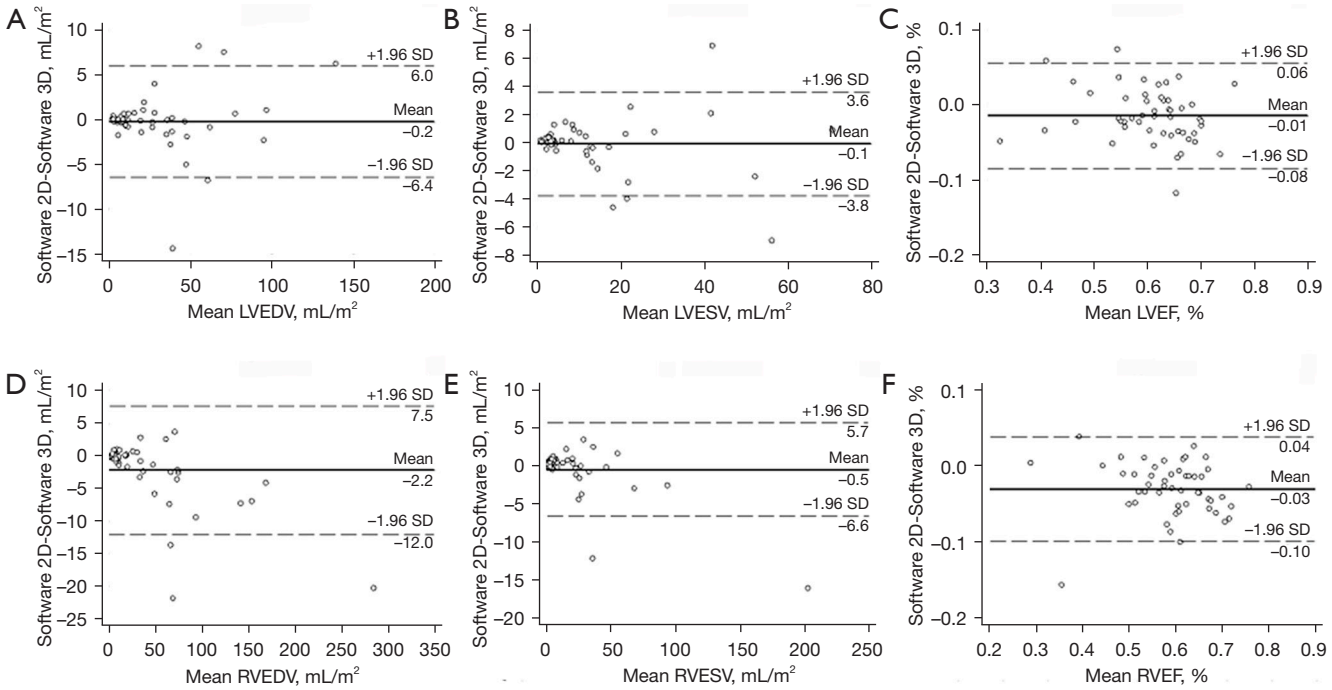

Figure 4 Comparison of Software^{2D} (Qmass) and Software^{3D} (Mimics) analysis of 4D MUSIC for measures of volumetry and function. Bland-Altman plots of (A) LVEDV, (B) LVESV, (C) LVEF, (D) RVEDV, (E) RVESV, and (F) RVEF. The mean values between 2D (Qmass) and 3D (Mimics) are on the x-axis and the absolute difference (Qmass-Mimics) are on the y-axis. LVEDV, left ventricular end-diastolic volume; LVESV, left ventricular end-systolic volume; LVEF, left ventricular ejection fraction; RVEDV, right ventricular end-diastolic volume; RVESV, right ventricular end-systolic volume; RVEF, right ventricular ejection fraction; MUSIC, multiphase, steady-state imaging with contrast.

Table 3 Correlation between 2D and 3D quantification of ventricular chamber volume and function for 4D MUSIC MRI

Variables	2D analysis†	3D analysis†	Spearman's rho	P value
LVEDV (mL/m^2)	17.8 (8.0–38.6)	17.5 (8.1–41.5)	0.99	<0.001
LVESV (mL/m^2)	5.5 (3.0–14.1)	5.4 (2.6–15.9)	0.99	<0.001
LVEF (%)	61.6 (56.4–65.2)	62.1 (56.7–68.4)	0.92	<0.001
RVEDV (mL/m^2)	18.4 (7.9–60.5)	18.4 (8.1–68.6)	0.99	<0.001
RVESV (mL/m^2)	6.1 (2.9–23.6)	5.40 (2.9–26.3)	0.99	<0.001
RVEF (%)	58.0 (53.7–64.6)	62.3 (53.3–66.3)	0.92	<0.001

†, values are reported as median and IQR. MUSIC, multiphase, steady-state imaging with contrast; MRI, magnetic resonance imaging; LVEDV, left ventricular end-diastolic volume; LVESV, left ventricular end-systolic volume; LVEF, left ventricular ejection fraction; RVEDV, right ventricular end-diastolic volume; RVESV, right ventricular end-systolic volume; RVEF, right ventricular ejection fraction; IQR, interquartile range.

Table 4 Intra- and inter-observer agreement of ventricular volumetry and function for 2D and 3D software platform analysis of 4D MUSIC MRI

Variables	Intra-observer 2D ICC (95% CI)	Inter-observer 2D ICC (95% CI)	Intra-observer 3D ICC (95% CI)	Inter-observer 3D ICC (95% CI)
LVEDV	1.00 (1.00–1.00)	1.00 (0.99–1.00)	1.00 (1.00–1.00)	1.00 (0.99–1.00)
LVESV	1.00 (1.00–1.00)	0.99 (1.00–1.00)	1.00 (0.99–1.00)	1.00 (0.99–1.00)
LVEF	0.99 (0.95–1.00)	0.95 (0.78–0.86)	0.97 (0.88–0.99)	0.96 (0.85–0.99)
RVEDV	1.00 (1.00–1.00)	0.99 (0.97–1.00)	1.00 (0.99–1.00)	1.00 (0.98–1.00)
RVESV	1.00 (0.99–1.00)	1.00 (0.98–1.00)	1.00 (0.98–1.00)	1.00 (0.98–0.99)
RVEF	0.98 (0.92–1.00)	0.92 (0.68–0.98)	0.95 (0.80–0.99)	0.96 (0.82–0.99)

MUSIC, multiphase, steady-state imaging with contrast; MRI, magnetic resonance imaging; ICC, intraclass correlation; LVEDV, left ventricular end-diastolic volume; LVESV, left ventricular end-systolic volume; LVEF, left ventricular ejection fraction; RVEDV, right ventricular end-diastolic volume; RVESV, right ventricular end-systolic volume; RVEF, right ventricular ejection fraction.

Table 5 Intra- and inter-observer variability for 2D software analysis of 4D MUSIC MRI

Variables	LVEDV	LVESV	LVEF	RVEDV	RVESV	RVEF
Intra-observer						
Mean difference ± SD†	−0.61±0.93	−0.30±0.64	0.95±1.38	0.16±2.15	−0.24±1.49	0.96±1.87
Limits of agreement†	−2.44 to 1.21	−1.55 to 0.95	−1.75 to 3.65	−4.05 to 4.37	−3.15 to 2.67	−2.71 to 4.63
Mean value ± SD†	31.11±27.17	13.40±14.47	61.01±8.19	38.46±27.79	15.63±13.05	61.65±7.26
CV (%)	2.92	5.57	1.99	3.18	6.69	2.37
Inter-observer						
Mean difference ± SD†	1.11±1.99	1.47±1.00	−3.20±3.78	6.26±6.14	2.06±2.25	0.40±4.37
Limits of agreement†	−2.78 to 5.00	−0.49 to 3.44	−10.34 to 3.95	−5.78 to 18.29	−2.35 to 6.46	−8.28 to 9.08
Mean value ± SD†	46.58±28.62	20.59±16.44	58.90±8.12	59.74±33.81	26.29±15.75	57.40±7.78
CV (%)	3.71	11.96	5.72	8.34	11.78	5.48

†, the unit for ventricular volume is mL/m^2, while the unit for ejection fraction is percent. MUSIC, multiphase, steady-state imaging with contrast; MRI, magnetic resonance imaging; LVEDV, left ventricular end-diastolic volume; LVESV, left ventricular end-systolic volume; LVEF, left ventricular ejection fraction; RVEDV, right ventricular end-diastolic volume; RVESV, right ventricular end-systolic volume; RVEF, right ventricular ejection fraction; SD, standard deviation; CV, coefficient of variation.

software over 2D software.

Intra- and interobserver reliability for quantification of volumetry and function by 4D MUSIC MRI

Two readers who regularly read cardiac MRI examinations independently reviewed and analyzed the same 10 cases. For both 2D and 3D software platforms, the intra- and interobserver reliability was excellent as evidenced by the high ICC, narrow 95% confidence interval (*Table 4*), and low CV (*Tables 5,6*). While all ICC were >0.9, with most approaching 0.99, the ICC tended to be higher for volume than EF. Moreover, values derived from the 3D software platform had higher ICC for both intra- and interobserver agreement (0.998, 0.998, respectively) than the 2D software (0.985, 0.997), respectively. The intraobserver variability was between 1.99–6.69% for 2D software, and between 3.85–7.97% for 3D software platforms. The interobserver variability was between 3.71–11.96% for 2D software, and between 4-9.38% for 3D software platforms.

Discussion

Our results demonstrate excellent accuracy and reliability using both 2D and 3D software platforms for quantification of ventricular volumes and function from 4D MUSIC

Table 6 Intra- and inter-observer variability for 3D software analysis of 4D MUSIC MRI

	LVEDV	LVESV	LVEF	RVEDV	RVESV	RVEF
Intra-observer						
Mean difference ± SD†	–0.31±2.01	0.43±1.99	–1.24±3.19	0.16±3.67	–0.24±1.83	0.96±4.12
Limits of agreement†	–4.25 to 3.63	–3.47 to 4.34	–7.50 to 5.01	–4.05 to 4.37	–3.15 to 2.67	–2.71 to 4.63
Mean value ± SD†	31.81±26.94	13.74±14.98	62.02±9.07	39.44±29.01	14.97±13.03	64.67 ±9.41
CV (%)	4.53	6.05	3.85	7.97	6.14	4.97
Inter-observer						
Mean difference ± SD†	–0.84±3.14	–0.86±2.22	0.94±3.26	–2.41±6.06	–0.47±2.64	–0.72±3.71
Limits of agreement†	–6.99 to 5.32	–5.22 to 3.50	–5.45 to 7.33	–14.28 to 9.46	–5.65 to 4.70	–7.98 to 6.55
Mean value ± SD†	50.67±28.45	23.91±17.81	56.28±8.31	69.65±38.33	29.70±18.10	59.32±8.82
CV (%)	6.11	9.38	4.00	6.25	5.34	4.96

†, the unit for ventricular volume is mL/m^2, while the unit for ejection fraction is percent. MUSIC, multiphase, steady-state imaging with contrast; MRI, magnetic resonance imaging; LVEDV, left ventricular end-diastolic volume; LVESV, left ventricular end-systolic volume; LVEF, left ventricular ejection fraction; RVEDV, right ventricular end-diastolic volume; RVESV, right ventricular end-systolic volume; RVEF, right ventricular ejection fraction; SD, standard deviation; CV, coefficient of variation.

MRI. Ventricular volumes and EF by 4D MUSIC MRI were comparable to those derived from reference bSSFP cine images. The current work further validates the clinical utility of ferumoxytol-enhanced MUSIC as a simplified 4D MRI approach by accurately and reliably enabling quantification of ventricular chamber volume and function using commercially available software.

Accuracy of volumetry and EF measurements is dependent on sharp delineation between blood pool and myocardium whereas reliability and agreement may be affected by discrimination of ventricles from great vessels and identification of the most basal slice. In our study, the trabeculae and papillary muscles were purposely excluded from the blood pool due to our use of semi-automatic thresholding. Secondly, with the use of ferumoxytol, the blood pool signal was very uniform and the contrast between blood pool and myocardium was excellent. The high spatial resolution achieved with 4D MUSIC enabled clear visualization of small structures, which were helpful in defining the contours for 3D volumetric and EF analysis.

Because 4D MUSIC images are cardiac phase-resolved and can be interrogated in any arbitrary imaging plane, the image dataset can be easily processed using 2D or 3D commercial software for quantification of volumetric and functional data. In our hands, both 2D and 3D image analysis software produced highly reliable biventricular volumetric and functional data. LV volume measurements were more precise with smaller mean differences as compared to RV volumes. We speculate that this is directly related to abnormal RV morphology in complex CHD and subjectivity in defining RV-RVOT border during semi-automatic image segmentation. The higher correlation for cine volumetry (r>0.95) compared to biventricular EF correlation (r=0.68–0.87) is likely due to variability in volumetric values (14). Our finding that 3D-derived volumetric measurements had higher inter and intra-observer agreement is concordant with published work demonstrating similar reproducibility with 3D relative to 2D imaging techniques (14,15). Prior work evaluating intra- and interobserver variability using bSSFP cine cardiac MRI in CHD reported intra-observer variability of 2.9–6.8% and interobserver variability of 2.9–10.2% (16).

Other approaches that have simplification of image acquisition as a similar goal exist (17-25) and include 4D flow MRI strategies (26-28). Relative to 4D MUSIC, the 4D flow approach offers additional information about flow. Other recent strategies take advantage of radial acquisitions with compressed sensing (23) whereby motion is handled by sorting acquired data into under-sampled motion states, which are then reconstructed into multidimensional and cardiac phase-resolved images. Building upon radial acquisition with compressed sensing reconstruction, a 5D whole-heart sparse MRI approach has also been described whereby acquired 3D k-space data are sorted into a

5D dataset containing separate respiratory and cardiac dimensions, which are then reconstructed into 3D cardiac phase-resolved images (25). These two latter strategies have not been tested in a patient population with heterogeneous and complex intra-cardiac anatomy and extra-cardiac vascular malformations such as complex CHD nor within the age range of 3 days to 18 years. To be comparable to 4D MUSIC, the newer radial acquisition with compressed sensing approaches will need to be tested under similar clinical scenarios and regardless of whether 2D or 3D commercial post-processing software is used, suitable measures of volumetry and function need to also be easily ascertained.

Overall, while our study demonstrates the accuracy and reliability of using 4D MUSIC to evaluate cardiac volumetry and function, there are limitations. One limitation of our study is the modest sample size of acquired conventional cine images (n=10 subjects). A second limitation is the spread in temporal resolution of the 4D MUSIC data. Whereas the temporal resolution of the multislice 2D SSFP cine was 40–60 ms, the temporal resolution of the 4D MUSIC was as low as 95 ms. In these patients, the clinical questions were about relationships in cardiovascular anatomy rather than regional wall motion or function. Nevertheless, it is reassuring that, even with modest temporal resolution, the volumetric measurements correlated well and were 1.5 to 3.9 mL/m^2 higher when compared to multislice 2D SSFP cine. Despite these limitations, we were able to show that measures of ventricular volume and function from 4D MUSIC MRI using commercially available software were similar to 2D SSFP cine, suggesting that 4D MUSIC may obviate the need to perform supplemental multislice 2D cine acquisition.

Conclusions

Highly accurate and reliable cardiac volumetry and function can be obtained using both 2D and 3D image software analysis of ferumoxytol-enhanced 4D MUSIC MRI for children with CHD. If validated in a multicenter setting and across a wider age range cohort, ferumoxytol-enhanced 4D MUSIC MRI may serve as the new standard for simplified cardiovascular MR image acquisition in pediatric CHD and replacing the conventional practice of multislice 2D image acquisition for anatomic and functional assessment.

Acknowledgments

Funding: This work was supported by the National Institutes of Health (No. R01HL127153 and No. R01HL148182).

Footnote

Reporting Checklist: The authors have completed the GRRAS reporting checklist. Available at https://qims.amegroups.com/article/view/10.21037/qims-21-1243/rc

Conflicts of Interest: All authors have completed the ICMJE uniform disclosure form (available at https://qims.amegroups.com/article/view/10.21037/qims-21-1243/coif). PH, JPF, TY and KLN report receiving grants support from the National Institutes of Health (No. R01HL127153 and No. R01HL148182). The other authors have no conflicts of interest to declare.

Ethical Statement: The authors are accountable for all aspects of the work in ensuring that questions related to the accuracy or integrity of any part of the work are appropriately investigated and resolved. The study was conducted in accordance with the Declaration of Helsinki (as revised in 2013). The study was approved by the Institutional Ethics Board at University of California, Los Angeles, USA. All patients or their legal guardians gave written informed consent.

References

1. Davlouros PA, Niwa K, Webb G, Gatzoulis MA. The right ventricle in congenital heart disease. Heart 2006;92 Suppl 1:i27-38.
2. Haddad F, Hunt SA, Rosenthal DN, Murphy DJ. Right ventricular function in cardiovascular disease, part I: Anatomy, physiology, aging, and functional assessment of the right ventricle. Circulation 2008;117:1436-48.

3. Fratz S, Chung T, Greil GF, Samyn MM, Taylor AM, Valsangiacomo Buechel ER, Yoo SJ, Powell AJ. Guidelines and protocols for cardiovascular magnetic resonance in children and adults with congenital heart disease: SCMR expert consensus group on congenital heart disease. J Cardiovasc Magn Reson 2013;15:51.
4. Han F, Rapacchi S, Khan S, Ayad I, Salusky I, Gabriel S, Plotnik A, Finn JP, Hu P. Four-dimensional, multiphase, steady-state imaging with contrast enhancement (MUSIC) in the heart: a feasibility study in children. Magn Reson Med 2015;74:1042-9.
5. Han F, Zhou Z, Han E, Gao Y, Nguyen KL, Finn JP, Hu P. Self-gated 4D multiphase, steady-state imaging with contrast enhancement (MUSIC) using rotating cartesian K-space (ROCK): Validation in children with congenital heart disease. Magn Reson Med 2017;78:472-83.
6. Zhou Z, Han F, Rapacchi S, Nguyen KL, Brunengraber DZ, Kim GJ, Finn JP, Hu P. Accelerated ferumoxytol-enhanced 4D multiphase, steady-state imaging with contrast enhancement (MUSIC) cardiovascular MRI: validation in pediatric congenital heart disease. NMR Biomed 2017;30:10.1002/nbm.3663.
7. Zhou Z, Han F, Yoshida T, Nguyen KL, Finn JP, Hu P. Improved 4D cardiac functional assessment for pediatric patients using motion-weighted image reconstruction. MAGMA 2018;31:747-56.
8. Moon JC, Lorenz CH, Francis JM, Smith GC, Pennell DJ. Breath-hold FLASH and FISP cardiovascular MR imaging: left ventricular volume differences and reproducibility. Radiology 2002;223:789-97.
9. Alfakih K, Plein S, Thiele H, Jones T, Ridgway JP, Sivananthan MU. Normal human left and right ventricular dimensions for MRI as assessed by turbo gradient echo and steady-state free precession imaging sequences. J Magn Reson Imaging 2003;17:323-9.
10. Michaely HJ, Nael K, Schoenberg SO, Laub G, Reiser MF, Finn JP, Ruehm SG. Analysis of cardiac function--comparison between 1.5 Tesla and 3.0Tesla cardiac cine magnetic resonance imaging: preliminary experience. Invest Radiol 2006;41:133-40.
11. Carr JC, Simonetti O, Bundy J, Li D, Pereles S, Finn JP. Cine MR angiography of the heart with segmented true fast imaging with steady-state precession. Radiology 2001;219:828-34.
12. Bashir MR, Bhatti L, Marin D, Nelson RC. Emerging applications for ferumoxytol as a contrast agent in MRI. J Magn Reson Imaging 2015;41:884-98.
13. Nguyen KL, Han F, Zhou Z, Brunengraber DZ, Ayad I, Levi DS, Satou GM, Reemtsen BL, Hu P, Finn JP. 4D MUSIC CMR: value-based imaging of neonates and infants with congenital heart disease. J Cardiovasc Magn Reson 2017;19:40.
14. Margossian R, Schwartz ML, Prakash A, Wruck L, Colan SD, Atz AM, Bradley TJ, Fogel MA, Hurwitz LM, Marcus E, Powell AJ, Printz BF, Puchalski MD, Rychik J, Shirali G, Williams R, Yoo SJ, Geva T; Pediatric Heart Network Investigators. Comparison of echocardiographic and cardiac magnetic resonance imaging measurements of functional single ventricular volumes, mass, and ejection fraction (from the Pediatric Heart Network Fontan Cross-Sectional Study). Am J Cardiol 2009;104:419-28.
15. Chuang ML, Hibberd MG, Salton CJ, Beaudin RA, Riley MF, Parker RA, Douglas PS, Manning WJ. Importance of imaging method over imaging modality in noninvasive determination of left ventricular volumes and ejection fraction: assessment by two- and three-dimensional echocardiography and magnetic resonance imaging. J Am Coll Cardiol 2000;35:477-84.
16. Luijnenburg SE, Robbers-Visser D, Moelker A, Vliegen HW, Mulder BJ, Helbing WA. Intra-observer and interobserver variability of biventricular function, volumes and mass in patients with congenital heart disease measured by CMR imaging. Int J Cardiovasc Imaging 2010;26:57-64.
17. Sørensen TS, Körperich H, Greil GF, Eichhorn J, Barth P, Meyer H, Pedersen EM, Beerbaum P. Operator-independent isotropic three-dimensional magnetic resonance imaging for morphology in congenital heart disease: a validation study. Circulation 2004;110:163-9.
18. Uribe S, Tangchaoren T, Parish V, Wolf I, Razavi R, Greil G, Schaeffter T. Volumetric cardiac quantification by using 3D dual-phase whole-heart MR imaging. Radiology 2008;248:606-14.
19. Henningsson M, Chan RH, Goddu B, Goepfert LA, Razavi R, Botnar RM, Schaeffter T, Nezafat R. Contrast-enhanced specific absorption rate-efficient 3D cardiac cine with respiratory-triggered radiofrequency gating. J Magn Reson Imaging 2013;37:986-92.
20. Pang J, Sharif B, Fan Z, Bi X, Arsanjani R, Berman DS, Li D. ECG and navigator-free four-dimensional whole-heart coronary MRA for simultaneous visualization of cardiac anatomy and function. Magn Reson Med 2014;72:1208-17.
21. Coppo S, Piccini D, Bonanno G, Chaptinel J, Vincenti G, Feliciano H, van Heeswijk RB, Schwitter J, Stuber M. Free-running 4D whole-heart self-navigated golden angle MRI: Initial results. Magn Reson Med 2015;74:1306-16.

22. Usman M, Ruijsink B, Nazir MS, Cruz G, Prieto C. Free breathing whole-heart 3D CINE MRI with self-gated Cartesian trajectory. Magn Reson Imaging 2017;38:129-37.
23. Liu J, Feng L, Shen HW, Zhu C, Wang Y, Mukai K, Brooks GC, Ordovas K, Saloner D. Highly-accelerated self-gated free-breathing 3D cardiac cine MRI: validation in assessment of left ventricular function. MAGMA 2017;30:337-46.
24. Moghari MH, Barthur A, Amaral ME, Geva T, Powell AJ. Free-breathing whole-heart 3D cine magnetic resonance imaging with prospective respiratory motion compensation. Magn Reson Med 2018;80:181-9.
25. Feng L, Coppo S, Piccini D, Yerly J, Lim RP, Masci PG, Stuber M, Sodickson DK, Otazo R. 5D whole-heart sparse MRI. Magn Reson Med 2018;79:826-38.
26. Cheng JY, Hanneman K, Zhang T, Alley MT, Lai P, Tamir JI, Uecker M, Pauly JM, Lustig M, Vasanawala SS. Comprehensive motion-compensated highly accelerated 4D flow MRI with ferumoxytol enhancement for pediatric congenital heart disease. J Magn Reson Imaging 2016;43:1355-68.
27. Cheng JY, Zhang T, Alley MT, Uecker M, Lustig M, Pauly JM, Vasanawala SS. Comprehensive Multi-Dimensional MRI for the Simultaneous Assessment of Cardiopulmonary Anatomy and Physiology. Sci Rep 2017;7:5330.
28. Hanneman K, Kino A, Cheng JY, Alley MT, Vasanawala SS. Assessment of the precision and reproducibility of ventricular volume, function, and mass measurements with ferumoxytol-enhanced 4D flow MRI. J Magn Reson Imaging 2016;44:383-92.

Cite this article as: Yoshida T, Chen JJ, Zhou B, Finn JP, Hu P, Nguyen KL. Ferumoxytol-enhanced 4D multiphase, steady-state imaging with magnetic resonance in congenital heart disease: ventricular volume and function across 2D and 3D software platforms. Quant Imaging Med Surg 2022;12(9):4377-4389. doi: 10.21037/qims-21-1243

